

# MIMO Channel Estimation for Time-Division Duplex Distributed Antenna Cooperative Transmission

Fumiyuki ADACHI, Amnart BOONKAJAY, Yuta SEKI and Tomoyuki SAITO

Research Organization of Electrical Communication (ROEC), Tohoku University

2-1-1 Katahira, Aoba-ku, Sendai, 980-8577 Japan

E-mail: adachi@eeci.tohoku.ac.jp, {amnart, seki.yuta, saito.tmm}@riec.tohoku.ac.jp

**Abstract**— We have been studying cooperative distributed antenna transmission (CDAT) as a promising technique for realizing the 5<sup>th</sup> generation (5G) high-speed mobile communications. Assuming time division duplex (TDD), the macro-cell base station (MBS) and the user equipments (UEs) conduct the channel estimation independently to obtain the shared channel state information (CSI). In this paper, we introduce a TDD frame structure consisting of uplink pilot time slot and downlink pilot time slot followed by data time slots. MIMO channel estimation is done before the user data transmission. Also presented is the pilot signal design. The accuracy of the proposed MIMO channel estimation and achievable bit error rate (BER) performance of user data transmission are evaluated by computer simulation.

**Keywords**—5G mobile communications system, distributed antenna, cooperative transmission, time-division duplex (TDD), channel estimation

## I. INTRODUCTION

The mobile communications networks have evolved their generation every 10 years. The first generation (1G) started in around 1980's and now the 4G (LTE-Advanced) is under a rapid deployment around the world. To enhance the mobile communications services, the research and development (R&D) of 5G networks is ongoing to initiate 5G services by 2020 [1]. In Japan, the R&D development funded by The Ministry of Internal Affairs and Communications (MIC) started in Sept. 2015 [2].

Enhanced mobile broadband services of over 1Gbps/user are expected in 5G. Significant improvement in the area spectrum efficiency (bps/Hz/km<sup>2</sup>) is necessary to provide enhanced mobile broadband services. Antenna technology may play an important role to achieve this target. The use of massive number of antennas is promising. The authors have been studying distributed antenna small-cell network, in which a number of antennas are deployed over a traditional macro-cell area [3]. Some distributed antennas close to each user equipment (UE) are cooperatively used for multi-input multi-output (MIMO) signal transmission. The MIMO signal transmission is carried out by means of either single-user space-time block coded transmit diversity (STBC-TD) or multi-user minimum mean square error filtering

combined with singular value decomposition (MMSE-SVD). This is called the cooperative distributed antenna transmission (CDAT) [4, 5].

For CDAT using MMSE-SVD, transmitting and receiving sides need to share the channel state information (CSI) for computing transmit and receive filtering weights. This should be done prior to data transmission in a transmission time interval (TTI). However, an LTE-Advanced frame format [6] allocates reference signals for channel estimation at the receiver only. This causes difficulty in the realization of CDAT since there is no CSI available for generating transmit filter. Most of literatures considering MIMO transmission using transmit precoder assume the perfect CSI [7]. Ref. [8] pointed out that a training phase is necessary for transmitting pilots and conducting channel estimation at transmitter and receivers before data transmission, but the subframe format was not discussed.

In this paper, we present a time-division duplex (TDD) subframe structure which realizes the pilot-assisted multi-input multi-output (MIMO) channel estimation based on the sparse channel structure observed in a distributed antenna small-cell network and also the pilot design which makes it possible to estimate a large scale MIMO channel. Frequency-division duplex (FDD) transmission is inappropriate since UE and the macro-cell base station (MBS) need to feedback the CSIs obtained by channel estimation to each other. On the other hand, when using TDD, exploiting the channel reciprocity, both MBS and UE can conduct the channel estimation independently to obtain the shared CSI without the necessity of feedback. To improve the transmission quality, it is helpful to inform the channel quality information (CQI) to the MBS. The accuracy of the proposed MIMO channel estimation and the achievable bit error rate (BER) performance of user data transmission are evaluated by computer simulation.

The rest of the paper is organized as follows. Sect. II overviews CDAT for distributed antenna small-cell network. In Sect. III, the MIMO channel estimation scheme and the pilot design are proposed. In Sect. IV, the simulation results on channel estimation error and achievable BER of user data transmission are presented and discussed. Sect. V offers some concluding remarks.

## II. OVERVIEW OF COOPERATIVE DISTRIBUTED ANTENNA TRANSMISSION

### A. Distributed antenna small-cell network

Cellular network design is based on the spatial reuse of the same frequency by allowing the co-channel interference (CCI) from other transmitters in order to improve the area spectrum efficiency [9]. A significant improvement of area spectrum efficiency is required for 5G mobile communication networks in order to provide enhanced mobile broadband, massive device connection, and ultra-reliable and low latency services. In addition to the area spectrum efficiency, the energy efficiency (bits/Joule) becomes an important issue since the higher the data rate becomes, the more transmit power is required (this is especially a big issue for battery-operated UEs).

The most effective approach to simultaneously improve both the area spectrum efficiency and energy efficiency is to adopt a small-cell structured network. By reducing the cell size, the frequency reuse distance can be shortened, thereby improving the area spectrum efficiency. At the same time, the transmit power can significantly be reduced and accordingly, the energy efficiency improves.

However, a straightforward approach may have a problem of frequent handover. This significantly increases the control signaling traffic for high mobility UEs. There are two approaches to avoid this handover problem [10, 11]: the one is so-called massive MIMO or centralized massive MIMO [12], where a large number of narrow beams are generated, each illuminates a different UE. The other is distributed massive MIMO [13] or distributed antenna small-cell network [3], in which a large number of antennas are deployed over a macro-cell area and some antennas close to a UE are chosen for signal transmission. By selecting appropriate distributed antennas, the shadowing impact can be mitigated and therefore, the communications quality can be further improved over a macro-cell area compared to the centralized massive MIMO.

The conceptual structure of distributed antenna small-cell network is illustrated in Fig. 1. All distributed antennas deployed in a macro-cell area are connected by optical fiber links to a MBS which is composed of baseband TRx signal processor and TRx controller. CDAT is an extension of coordinate multi-point (CoMP) transmission of LTE-Advanced [14]. Similar to the centralized massive MIMO network, scheduling (antenna selection, UE selection, and resource allocation) can be done at an MBS. In massive MIMO networks, the handover can be replaced with beam or antenna selection within MBS which is much easier to implement.

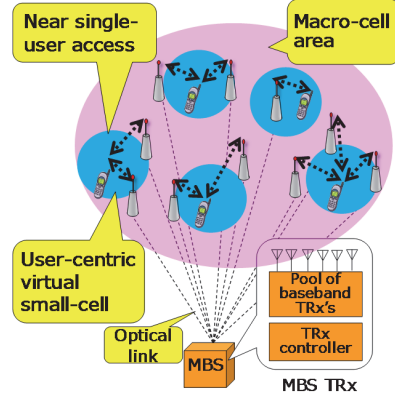


Fig. 1. Conceptual structure of distributed antenna small-cell network (only single macro-cell area covered by a MBS is shown).

### B. CDAT techniques

A broadband radio channel of >100 MHz bandwidth becomes significantly frequency-selective. Powerful equalization technique needs to be adopted. The well-known frequency-domain equalization (FDE) [15, 16, 17] can be used. The CSI is necessary for the equalization. If time-division duplex (TDD) is used, the channel reciprocity between the uplink (UE→MBS) and downlink (MBS→UE) can be exploited. Based on the above discussion, the shared CSI is obtained by letting MBS and UE independently estimate the channel, while no CSI feedback is necessary unlike in FDD.

The authors have been studying the CDAT techniques with both transmit and receive FDE at MBS side (see Fig.2). CDAT includes single-user STBC-TD [18, 19] and multi-user MMSE-SVD [4, 5]. Some distributed antennas near a UE are selected for performing CDAT. Multi-user MMSE-SVD is used to improve the throughput when UE is in a good channel condition. When UE is in a poor channel condition, single-user STBC-TD can be used.

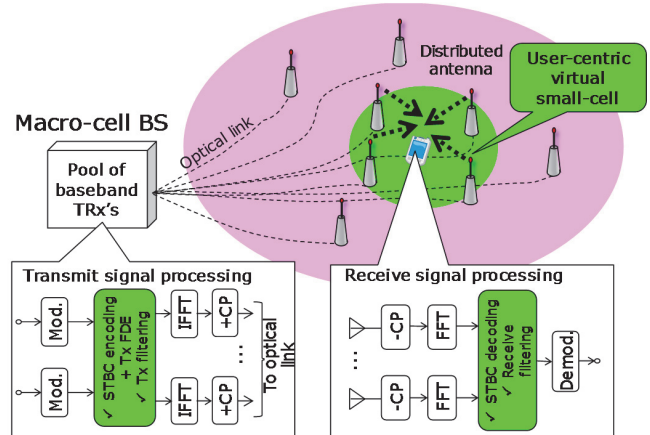


Fig. 2 CDAT for OFDM downlink.

### III. MIMO CHANNEL ESTIMATION

When using CDAT, accurate estimation of MIMO channel between distributed antennas and UEs is necessary. Assuming the perfect CSI, we have studied the transmission performances of single-user STBC-TD and multi-user MMSE-SVD [4, 5]. For single-user STBC-TD, maximal ratio transmit (MRT)-FDE [20, 21] and MMSE-receive FDE [22, 23] are used at MBS. On the other hand, multi-user MMSE-transmit FDE and MMSE-receive FDE are used at MBS for multi-user MMSE-SVD (note that the eigenmode reception and transmission are used at UE). Therefore, before the downlink/uplink transmission of user data, the CSI of MIMO channel must be acquired at both MBS and UEs.

In this paper, similar to LTE-Advanced, we assume orthogonal frequency division multiplexing (OFDM) downlink and single-carrier (SC) uplink. Furthermore, assuming TDD transmission and exploiting the channel reciprocity, we propose a MIMO channel estimation which requires no feedback of the CSI estimates obtained by UEs (MBS) to MBS (UEs). Both MBS and UEs can perform the channel estimation independently to acquire the shared CSIs.

#### A. Subframe structure

The subframe structure supporting MIMO channel estimation is illustrated in Fig. 3. One subframe consists of the uplink pilot time slot (UpPTS) and the downlink pilot time slot (DwPTS) followed by 12 data time slots (DTSS). The transmission efficiency of user data rate is kept the same as 3GPP Rel.10 subframe structure [24]. Each TS length is equal to one OFDM symbol plus cyclic prefix (CP) length.

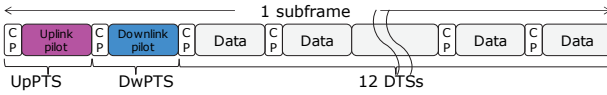


Fig. 3 Subframe structure.

#### B. Pilot design

The following three design requirements are considered.

*Req.1:* As many channels as possible should be simultaneously estimated without distortion.

*Req.2:* Pilot signal should have as low peak-to-average power ratio (PAPR) as possible.

*Req.3:* Transmission of the CQI (e.g., CCI level) together with pilot during UpPTS and DwPTS is desirable. If UE can inform its downlink CQI to MBS, MBS can adapt the downlink transmission to the CCI level at UE.

Two orthogonal pilot signal designs are considered: Frequency-division multiplex (FDM) pilot signal design and delay-time division multiplex (DTDM) pilot signal design. Both designs exploit the sparse channel structure which is observed in a small-cell network. Assume that the channel maximum time delay  $\tau_{\max}$  normalized by the subcarrier

separation is much smaller than the number  $N_c$  of subcarriers. Minimum required number of channel samples over the signal bandwidth of  $N_c$  subcarriers is  $\tau_{\max}$  according to the Nyquist sampling theory. Hence, as many as  $N_c/\tau_{\max} (>>1)$  channels can be simultaneously estimated without distortion. Pilot signals are generated according to the following two pilot signal designs.

*FDM pilot signal:* equally spaced  $\tau_{\max}$  subcarriers are used out of  $N_c$  subcarriers for estimating one channel as shown in Fig. 4. A total of  $N_c/\tau_{\max}$  orthogonal pilot signals can be generated.

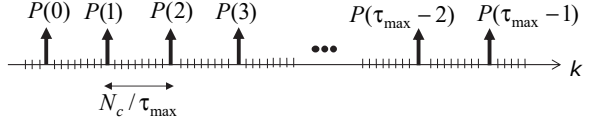


Fig. 4 FDM pilot.

*DTDM pilot signal:*  $N_c$ -symbol time-domain mother pilot signal is generated first. Then, a total of  $N_c/\tau_{\max}$  orthogonal pilot signals are generated by cyclic-shifting the mother pilot signal in time-domain. The amount of cyclic shift should be an integer multiple of  $\tau_{\max}$ . A different cyclic shift is used to estimate a different channel. In Fig. 5, a pilot signal with a cyclic shift of  $m$  integer multiple of  $\tau_{\max}$  is shown.

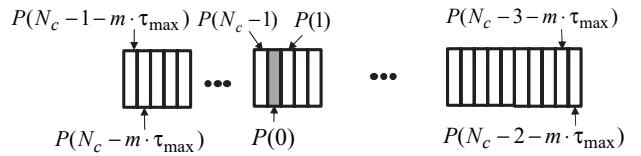


Fig. 5 DTDM pilot which is a cyclic shifted ( $m \cdot \tau_{\max}$  cyclic delay) version of the mother pilot signal.

Let us assume that  $N_{\text{macro}}$  distributed antennas are deployed in a macro-cell area and each UE is equipped with  $N_{\text{ue}}$  antennas. Assuming  $N_c=1024$  subcarriers and  $\tau_{\max}=16$ , each UE can estimate  $64 \times N_{\text{ue}}$  MIMO channel between  $N_{\text{macro}}=64$  distributed antennas and  $N_{\text{ue}}$  UE antennas. On the other hand, MBS can simultaneously estimate  $N_{\text{macro}} \times 64$  MIMO channel between  $N_{\text{macro}}$  distributed antennas and  $U=64/N_{\text{ue}}$  UEs (i.e., a total of 64 UE antennas). Channel estimation can be done using delay-time domain windowing technique [25, 26].

Requirement 2 can be met if the Zadoff-Chu sequence  $P_i(k)$  [27] having the constant amplitude property in both time-domain and frequency-domain is used as the pilot.  $P_i(k)$  is given as

$$P_i(k) = \exp(jk^2 i\pi / N_p) \text{ for } k=0 \sim N_p-1, \quad (1)$$

where  $N_p$  denotes the total number of pilot subcarriers,  $k$  denotes the subcarrier index, and  $i$  denotes a positive integer which is relatively prime to  $N_p$ . If  $N_p=\tau_{\max}$  subcarriers are

modulated by Zadoff-Chu sequence, the resultant time-domain pilot has a constant amplitude.

Requirement 3 can be met if the number of transmit antennas is less than or equal to  $N_c/\tau_{\max}$ . Below, OFDM simultaneous pilot/CQI transmission is presented. The number  $N_{\text{CQI}}$  of CQI symbols (subcarriers) is given as  $N_{\text{CQI}} = N_c / N_t - N_p$  for OFDM, where  $N_t$  represents the number of transmit antennas, given as  $N_t = N_{\text{ue}} \times U$  for uplink and  $N_t = N_{\text{macro}}$  for downlink, and  $N_p \geq \tau_{\max}$ . Assuming  $N_c = 1024$ ,  $\tau_{\max} = 16$ , and  $N_t = 32$ ,  $U = 16$  UEs can transmit  $\tau_{\max} = 16$ -symbol pilot and  $N_{\text{CQI}} = 16$ -symbol CQI simultaneously to MBS from each of  $N_{\text{ue}} = 2$  antennas. On the other hand, MBS can transmit  $\tau_{\max} = 16$ -symbol pilot and  $N_{\text{CQI}} = 16$ -symbol CQI simultaneously to UEs from each of  $N_{\text{macro}} = 32$  distributed antennas. However, this OFDM simultaneous pilot/CQI transmission has high PAPR.

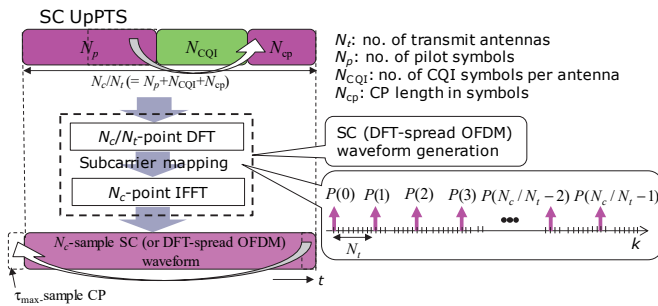


Fig. 6 SC pilot structure for simultaneous transmission of pilot and CQI.

To avoid the PAPR increase, SC simultaneous pilot/CQI transmission is used, which is illustrated in Fig. 6.  $N_{\text{CQI}}$  is given as  $N_{\text{CQI}} = N_c / N_t - N_p - N_{\text{cp}}$  for SC, where  $N_{\text{cp}} (= \tau_{\max})$  is the CP length (in symbols). The last  $N_{\text{cp}}$ -symbol part of pilot is copied and is inserted as CP at the end of CQI data in order to avoid the pilot contamination caused by the inter-symbol interference (ISI) from CQI data to pilot. Therefore, the value of  $N_t$  must be set smaller than for the case of OFDM simultaneous pilot/CQI transmission. Assuming  $N_c = 1024$ ,  $\tau_{\max} = 16$ , and  $N_t = 16$ , we have  $N_{\text{cp}} = 16$  and  $N_{\text{CQI}} = 48 - N_p$ , where  $N_p \geq 16$ . The channel estimation and the CQI detection can be done at MBS receiver as follows (see Fig. 7).

*Step 1:* channel estimation by using the pilot only.

*Step 2:* equalization and CQI detection.

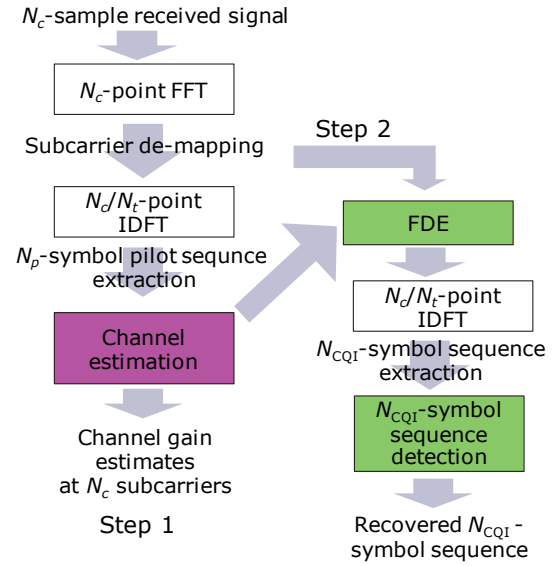


Fig. 7 Channel estimation and CQI detection.

#### IV. COMPUTER SIMULATION

##### A. Simulation setting

A single macro-cell model is assumed. The propagation channel is assumed to have a path loss exponent of  $\alpha = 3.5$  and is modeled as a frequency-selective Rayleigh channel having  $L = 16$ -path uniform power delay profile and the maximum delay time  $\tau_{\max} = 16$ . In the macro-cell area,  $N_{\text{macro}} = 32$  distributed antennas and  $U = 16$  UEs, each equipped with  $N_{\text{ue}} = 2$  antennas, are randomly distributed.

OFDM downlink and SC uplink transmissions are assumed. Pilot is generated using Zadoff-Chu sequence and 16QAM modulation is used for CQI and user data transmissions.  $32 \times 32$  MIMO channel estimation is done using the delay time domain windowing technique. The best channel is selected among  $32 \times 32$  MIMO channel for single transmit antenna and single receive antenna (SISO) transmission of user data.

##### B. Channel estimation accuracy

The normalized mean square error (NMSE) is measured and the distribution of NMSE is obtained. The average NMSE is plotted as a function of the received pilot subcarrier energy-to-the AWGN power spectrum density ratio,  $E_s/N_0$ , in Fig. 8.

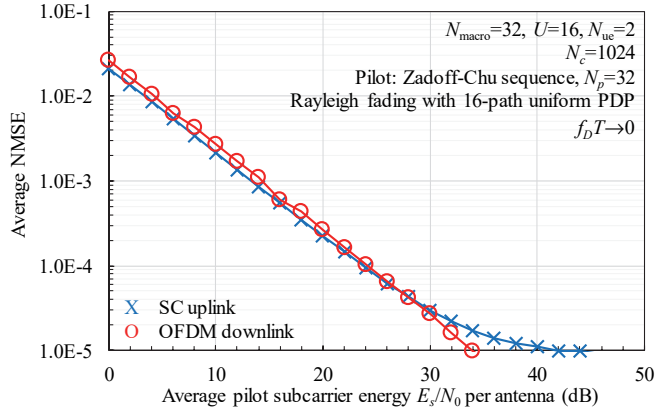


Fig. 8 Average NMSE performance.

Both SC uplink pilot and OFDM downlink pilot achieve similar channel estimation accuracy. However, the SC uplink pilot provides a slightly better channel estimation. This is due to the fact that SC can take an advantage of frequency-selectivity of the channel and obtain the frequency diversity effect. On the other hand, a floor value is observed in a high  $E_s/N_0$  region for SC pilot case. This is because of ISI caused by the channel frequency-selectivity. It will be confirmed in the next subsection that the MSE floor in SC pilot case does not result in a significant BER performance degradation since the MSE value is quite small.

### C. BER of user data transmission

The uncoded BER of SC uplink at each random location of UE is measured by computer simulation. A total of 1024  $\times$  12 symbols are transmitted during 12 DTSs. The pilot transmit power is set the same as the user data transmission power. Transmit or receive MMSE-FDE is used at MBS side. The SC MMSE weight for the  $k$ th subcarrier is given as [28]

$$W_{\text{MMSE}}(k) = A \times \hat{H}^*(k) / [\hat{H}(k)]^2 + (E_s / N_0)^{-1}, \quad (2)$$

where  $A$  denotes the power normalization factor (for receive MMSE-FDE,  $A$  can be an arbitrary positive number) and  $\hat{H}(k)$  denotes the estimated channel transfer function.

The macro-cell area average uncoded BER is plotted in Fig. 9 as a function of the normalized transmit  $E_s/N_0$  assuming a quasi-static fading environment (i.e., the maximum Doppler frequency  $f_D \rightarrow 0$ ). For comparison, the BER performance with perfect CSI is also plotted. The comparison between SC uplink with receive MMSE-FDE and OFDM downlink shows that our proposed MIMO channel estimation provides BER performance almost identical to the perfect CSI.

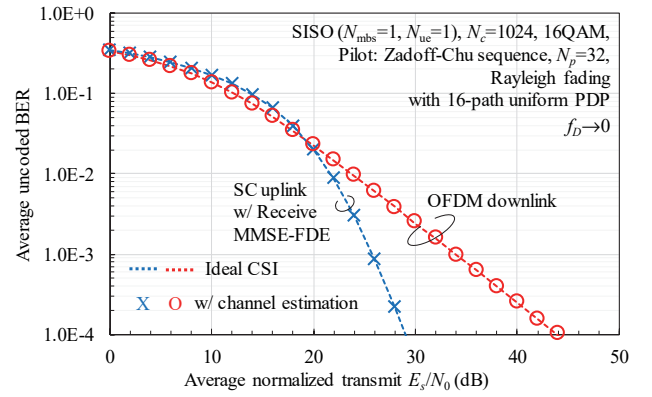


Fig. 9 Macro-cell area average uncoded BER performance.

Using the subframe structure shown in Fig. 3, the receive MMSE-FDE weight constructed by the estimated CSI is already old when receiving the user data. Therefore, if the channel changes rapidly, the time difference between when the CSI is acquired and when the CSI is used cannot be neglected. The impact of the normalized maximum Doppler frequency  $f_D T$  on the BER averaged over 12 DTSs is plotted in Fig. 10, where  $T$  denotes the TS length. Average BER starts to increase at  $f_D T = \text{around } 5 \times 10^{-4}$ . Assuming the subcarrier spacing of 75kHz and the CP length of 1.67μs, the TS length becomes  $T = 14.97\mu\text{s}$ . This means that  $f_D T = 5 \times 10^{-4}$  corresponds to a UE mobility of 7.2 km/h if 5GHz carrier frequency is used.

To avoid the BER degradation in a high mobility environment, a technique to update the estimated CSI and/or MMSE-FDE weight during data transmission is necessary. The above problem is left as our important future study.

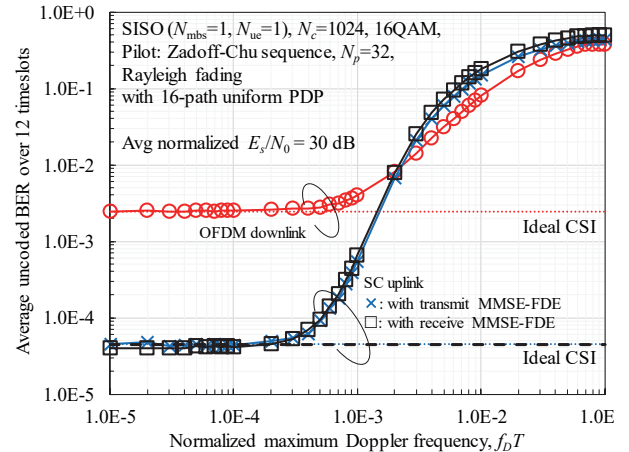


Fig. 10 Average BER versus  $f_D T$ .

## V. CONCLUSIONS

For CDAT, both transmitter and receiver need to share the CSI. Assuming TDD transmission, we proposed a

MIMO channel estimation technique which allows MBS and UEs to conduct the channel estimation independently in order to share the CSI without feedback. We presented a TDD frame structure consisting of UpPTS and DwPTS followed by 12 DTSSs. We also presented the pilot signal design achieving low PAPR and allowing simultaneous transmission of pilot and CQI. By exploiting the sparse channel structure observed in a small-cell network, channel estimation using delay-time domain windowing technique was presented. It was confirmed by computer simulation that the BER close to the perfect CSI case is achieved if the pilot power is set to be the same as that of user data transmission.

Improving the robustness against high mobility of UEs remains as our important future study.

#### ACKNOWLEDGMENT

The results presented in this paper have been achieved by “The research and development project for realization of the fifth-generation mobile communications network” commissioned to Tohoku University by The Ministry of Internal Affairs and Communications (MIC), Japan.

#### REFERENCES

- [1] C.-X. Wang, F. Haider, and X. Gao, “Cellular architecture and key technologies for 5G wireless communication networks,” IEEE Commun. Mag., Vol. 52, Issue 2, pp. 122-130, Feb. 2014.
- [2] [http://www.soumu.go.jp/menu\\_news/s-news/01kiban09\\_02000169.html](http://www.soumu.go.jp/menu_news/s-news/01kiban09_02000169.html). (in Japanese, 4 Aug. 2015)
- [3] F. Adachi, W. Peng, T. Obara, T. Yamamoto, R. Matsukawa, and M. Nakada, “Distributed antenna network for gigabit wireless access,” International Journal of Electronics and Communications (AEUE), Vol. 66, Issue 6, pp.605-612, 2012.
- [4] F. Adachi, S. Kumagai, H. Miyazaki, A. Boonkajay, Y. Seki, and T. Saito, “Distributed antenna cooperative signal transmission and signal peak suppression for 5G mobile communication systems,” IEICE Technical Report (in Japanese), Vol. 116, No. 110, RCS2016-73, pp. 159-164, June 2016.
- [5] F. Adachi, A. Boonkajay, Y. Seki, T. Saito, S. Kumagai, and H. Miyazaki, “Cooperative distributed antenna transmission for 5G mobile communications Network,” IEICE Trans. Commun., Vol. 100-E, No. 8, Aug. 2017.
- [6] 3GPP, R1-1610079, “Views on RS for demodulation and tracking,” NTT DOCOMO, INC., Oct. 2016.
- [7] H. Nishimoto, A. Taira, H. Iura, S. Uchida, A. Okazaki and A. Okumura, “NL-BMD: Nonlinear block multi-diagonalization precoding for high SHF wide-band massive MIMO in 5G,” IEICE Trans. Commun., Vol. 100-E, No. 8, Aug. 2017.
- [8] S. A. Banani, A. Rafiee and R. G. Vaughan, “Sum capacity of block-diagonalized multiuser MIMO downlink with channel estimation and finite-rate CSI feedback link,” Proc. 2016 IEEE 84th Vehicular Technology Conference (VTC-Fall), Montreal, Canada, 18-21 Sept. 2016.
- [9] W.C. Jakes, Jr. (Ed.), *Microwave Mobile Communications*, Wiley, New York, 1974.
- [10] F. Adachi, “Challenges toward spectrum-energy efficient mobile wireless networks,” IEICE Technical Report (in Japanese), Vol. 115, No. 123, CS2015-19, p. 55, July 2015.
- [11] A. A. M. Saleh, A. J. Rustako, and R. S. Roman, “Distributed antennas for indoor radio communications,” IEEE Trans. Commun., Vol. 35, No.12, pp. 1245-1251, Dec. 1987.
- [12] NTT DOCOMO White paper, July 2014 ([https://www.nttdocomo.co.jp/english/corporate/technology/whitepaper\\_5g/](https://www.nttdocomo.co.jp/english/corporate/technology/whitepaper_5g/)).
- [13] Y. Zhang, H. Hu, and J. Lao, *Distributed Antenna Systems: Open Architecture for Future Wireless Communications*, Auerbach Pub., 2007.
- [14] M. Sawahashi, Y. Kishiyama, A. Morimoto, D. Nishikawa, and M. Tanno, “Coordinated multipoint transmission/reception techniques for LTE-advanced [coordinated and distributed MIMO],” IEEE Wireless Commun., Vol. 17, Issue 3, pp.26-34, June 2010.
- [15] D. Falconer, S. L. Ariyavisitakul, A. Benyamin-Seeyar and B. Edison, “Frequency domain equalization for single-carrier broadband wireless systems,” IEEE Commun. Mag., Vol. 40, No. 4, pp. 58-66, Apr. 2002.
- [16] H. Sari, G. Karam, and I. Jeanclaude, “Transmission techniques for digital terrestrial TV broadcasting,” IEEE Commun. Mag., Vol. 33, pp. 100-109, Feb. 1995.
- [17] F. Adachi, D. Garg, S. Takaoka, and K. Takeda, “Broadband CDMA techniques,” IEEE Wireless Commun. Mag., Vol. 12, No. 2, pp. 8-18, April 2005.
- [18] S. M. Alamouti, “A simple transmit diversity technique for wireless communications,” IEEE J. Sel. Areas Commun., Vol. 16, No. 8, pp. 1451-1458, Oct. 1998.
- [19] V. Tarokh, H. Jafarkhani, and A. R. Calderbank, “Space-time block codes from orthogonal designs,” IEEE Trans. on Inform. Theory, Vol. 45, No. 5, pp. 1456-1467, July 1999.
- [20] H. Tomeba, K. Takeda, and F. Adachi, “Space-time block coded-joint transmit/receive antenna diversity using more than 4 receive antennas,” Proc. 2008 IEEE 68th Vehicular Technology Conference (VTC-Fall), Calgary, Canada, 21-25 Sept. 2008.
- [21] T. K. Y. Lo, “Maximum ratio transmission,” IEEE Trans. Commun., vol. 47, pp. 1458-1461, Oct. 1999.
- [22] K. Takeda, T. Itagaki, and F. Adachi, “Application of space-time transmit diversity to single-carrier transmission with frequency-domain equalization and receive antenna diversity in a frequency-selective fading channel,” IEE Proc.-Commun., vol. 151, No.6, pp. 627-632, Dec. 2004.
- [23] J. M. Auffray and J. F. Helard, “Performance of multicarrier CDMA technique combined with space-time block coding over Rayleigh channel,” Proc. IEEE Seventh International Symposium on Spread Spectrum Techniques and Applications, Vol. 2, pp. 348-352, Sept. 2002.
- [24] E. Dahlman, S. Parkvall and J. Skold, *4G: LTE-Advanced Pro and the Road to 5G*, 3rd-ed., Elsevier, 2016.
- [25] J. J. van de Beek, O. Edfors, M. Sandell, S. K. Wilson, and P. O. Borjesson, “On channel estimation in OFDM systems,” Proc. IEEE Veh. Technol. Conf. (VTC1995), Chicago, USA, Vol. 2, pp. 815-819, July 1995.
- [26] T. Fujimori, K. Takeda, K. Ozaki, A. Nakajima, and F. Adachi, “Channel estimation using cyclic delay pilot for SC-MIMO multiplexing,” IEICE Trans. Commun., Vol.E91-B, No.09, pp. 2925-2932, Sept. 2008.
- [27] D. C. Chu, “Polyphase codes with good periodic correlation properties,” IEEE Trans. Inf. Theory, Vol. 8, No. 4, pp. 531-532, July 1972.
- [28] A. Chouly, A. Brajal, and S. Jourdan, “Orthogonal multicarrier techniques applied to direct sequence spread spectrum CDMA system,” Proc. IEEE Globecom 1993, pp. 1723-1728, Houston, USA, Nov. 29 Nov. - 2 Dec. 1993.